

A Novel Closed-form Solution for Transverse Tensile Strength of **Polymer Composites based on Virtual Testing**

Sagar Shah*, Marianna Maiarù[†] University of Massachusetts Lowell, Lowell, MA, 01854

Evaluating the transverse tensile response of Polymer Matrix Composite (PMCs) is an extremely challenging problem since it is greatly influenced by the stress concentration induced within the composite microstructures by random fiber inclusions. This study presents a novel methodology to develop a closed-form solution for transverse composite strength prediction. A computational micromechanical study of composite microstructures with varying fiber volume fraction is carried out to accurately predict their transverse strength. Local stress concentration in composites due to fiber inclusion is investigated and a global stress concentration factor for each analyzed microstructure is quantified using statistical descriptor. Transverse composite strengths from FE simulations are expressed as a function of the constituent properties and the global stress concentration factors to derive a material specific closed-form relation.

I. Introduction

POLYMER Matrix Composites (PMCs) are widely used as primary load carrying materials in many engineering applications due to their desirable properties [1]. Desirable properties [1]. applications due to their desirable properties [1]. Despite their popularity, predicting their matrix-dominated transverse response is extremely challenging. Typically, complex and expensive experimental campaigns are carried out to test and characterize the mechanical response of PMCs under various loading conditions. More recently though, high-fidelity computational micromechanical models are being recognized as the preferred choice for virtual design and analysis of PMCs.

Computational micromechanical models are powerful tools that aid in establishing length scale-specific correlations, optimizing composite manufacturing, and designing better performing parts. However, there is a rising demand for robust analytical tools that enable virtual design and optimization of composite materials in a time and cost-effective manner [2]. Computational micromechanical models can facilitate the development of precise and accurate analytical closed-form solution for composite property predictions. Within the micromechanical framework, local stress and strain microfields are solved which provide valuable insights into constituent fiber/matrix interaction and its influence on the bulk composite response. This knowledge can be leveraged to establish phenomenological correlations and improve the accuracy of analytical models for composite property predictions.

A review of the literature presents several enhanced analytical models, such as the continuous periodic fiber model (CPFM), Chamis model and Bridging model, that can accurately predict the composite transverse stiffness [3–8]. However, similar estimations for the transverse tensile strength are particularly challenging. Limited studies have reported closed-form relations that can predict the transverse strength of composite from its constituent fiber/matrix properties [9–12]. Vignoli et al. [9] developed an elasticity-based solution and combined it with a modified Chamis model to predict transverse composite strength. The model predicted the transverse strength with 72% accuracy. A review of the existing models was carried out by Lupas et al. [12]. They reported similarly inaccurate model predictions for transverse strength. The transverse tensile strength not only depends on the constituent fiber/matrix properties but also on the fiber architecture and the variations in the microstructure, which induce stress concentration and drive failure within the composite microstructure [9, 13, 14]. The inability of current closed-form solutions to account for such variations results in inaccurate predictions. Expressing the transverse composite strength as a function of the constituent properties and the geometrical variations in the microstructure will establish the necessary dependencies required to develop a reliable and accurate closed-form relation.

The objective of this research is to present a unique numerical approach to develop a closed-form solution for transverse composite strength prediction. In this study, finite element (FE) based, computational micromechanical models are developed to analyze a wide array of composite microstructures for their transverse composite strengths. A

^{*}Ph.D. Student, Department of Mechanical Engineering.

[†]Corresponding author, Assistant Professor, Department of Mechanical Engineering.

stress concentration factor (SCF), which is greatly influenced by the fiber arrangement, is introduced and quantified for the analyzed composite microstructures. Statistical descriptors are developed to quantify the geometrical variations in these composite microstructures and correlate them to the SCF. Subsequently, transverse composite strengths from FE simulations are expressed as a function of the constituent properties and the SCF to derive the closed-form relation. The detailed approach and results are discussed in the following sections.

II. Computational Micromechanics

Recent advances in computing capabilities have facilitated the emergence of the field of computational micromechanics. Within this framework, representative volume elements (RVEs) of composite microstructures, subjected to various mechanical loading conditions, are analyzed and their microscale response are accurately predicted [15]. In the present study, a series of composite microstructures, with varying fiber volume fraction and random fiber arrangement, are analyzed for their transverse composite strength. The procedure to generate composite microstructures is discussed in Section II.A. The virtual mechanical loading analysis procedure and results for these microstructures are presented in Section II.B.

A. Modeling of Composite Microstructures

Random fiber arrangement, variation in the local fiber volume fraction and fiber-to-fiber proximity are widely recognized to induce stress concentration within a composite microstructure [10, 13, 14, 16, 17]. To accurately capture these mechanisms, which greatly influence the transverse composite response, microstructures comprising of randomly packed fibers with varying fiber volume fractions were modeled. Several strategies to generate composite microstructures with random fiber arrangement can be found in the literature [13, 18–30]. For this study, a random microstructure generator was developed in-house with MATLAB [31] and used to generate FE models with varying fiber volume fractions. For a given fiber diameter d_f , fiber volume fraction v_f and number of fibers n_f , the algorithm generated randomly distributed fiber centers. The fiber coordinates were then imported into Abaqus where the composite microstructure was modeled, discretized and appropriate boundary conditions were applied.

For the present study, composite microstructures consisted of 20 glass fiber inclusions ($d_f = 14 \mu m$) randomly dispersed in an epoxy matrix. The bonding between the fiber and the matrix was considered perfect. Several microstructures with varying fiber volume fraction ($0.24 \le v_f \le 0.6$), as illustrated in Figure 1a, were evaluated. To improve the prediction accuracy and account for statistical variations, five distinct realizations with random fiber arrangement were analyzed for each value of v_f . Five realizations of a 20 fiber composite microstructure with a $v_f = 0.55$ are shown in Figure 1b. Due to their nature, the constituent glass fibers and matrix were modeled as isotropic solids. Failure was admissible in the matrix material once the maximum principal stresses exceeded its critical strength. This was implemented in FE solver Abaqus/EXPLICIT, supplemented by user-written subroutine VUMAT. The mechanical properties for the glass fiber and the epoxy matrix used in this study are listed in Table 1.

Table 1 Constituent mechanical properties for virtual mechanical analysis.

(a) E-glass fiber

(b) Epoxy resin

Property		Value	Unit		Property		Value	Unit
Density	$ ho^{ m f}$	2550	$[kg/m^3]$		Elastic Modulus	E^{m}	2482	[MPa]
Elastic Modulus	$E_{11}^{\rm f} = E_{22}^{\rm f} = E_{33}^{\rm f}$	73000	[MPa]		Poisson's ratio	ν^{m}	0.37	[-]
Poisson's ratio	$v_{12}^{\rm f} = v_{13}^{\rm f} = v_{23}^{\rm f}$	0.22	[-]		Critical Strength	$\sigma_{\mathrm{cr}}^{\mathrm{m}}$	64.1	[MPa]
Shear Modulus	$G_{12}^{\mathrm{f}} = G_{13}^{\mathrm{f}} = G_{23}^{\mathrm{f}}$	30000	[MPa]		Fracture Toughness	$G_{ m IC}^{ m m}$	0.001	$[J/m^2]$

B. Virtual mechanical loading

The composite microstructures generated in the Section II.A were subjected to transverse mechanical loads by prescribing a velocity boundary condition shown in Figure 2. The objective here was to compute the transverse composite strength of the generated microstructures as a function of their fiber volume fraction. To model matrix failure in the microstructures, a progressive damage model [32], based on the theory of crackband [33], was implemented. The

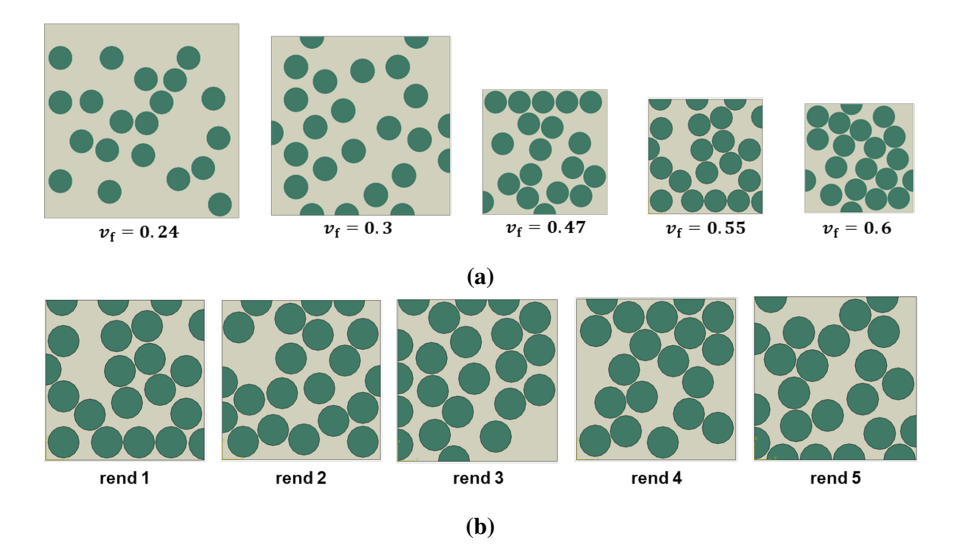


Fig. 1 Various realizations of the composite microstructures generated by the random microstructure generator: (a) shows the several fiber volume fractions v_f of microstructures considered in this study and (b) show five distinct renditions of a 20 fiber composite microstructure ($v_f = 0.55$).

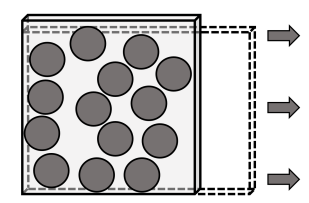


Fig. 2 Schematic of the prescribed boundary conditions during the virtual mechanical loading analysis.

maximum principal stress criterion was utilized to determine failure initiation in the matrix. The traction-separation law, which is governed by the fracture energy, was employed to define the post-peak softening behavior of the damaging material once the critical fracture stress was reached. The critical mode I energy release rate $G_{\rm IC}$ was given by

$$G_{\rm IC} = h^{\eta} \int_0^{\bar{\epsilon}_{\rm f}^{\eta}} \bar{\sigma}_{11}^{\eta} \,\bar{\epsilon}_{11}^{\eta} \,\mathrm{d}\bar{\epsilon} \tag{1}$$

where $\bar{\sigma}_{11}^{\eta}$ and $\bar{\epsilon}_{11}^{\eta}$ are the maximum principal stress and strain values in element η respectively, $\bar{\epsilon}_{\rm f}^{\eta}$ is the value of $\bar{\epsilon}_{11}^{\eta}$ which corresponds to a zero stress state on the post-peak stress versus strain plot, h^{η} is the characteristic length of the element η that preserves mesh objectivity by prescribing a normalized value of $G_{\rm IC}$ for each element, such that $g_{\rm IC}^{\eta} = G_{\rm IC}/h^{\eta}$.

A scalar damage factor D^{η} was computed to degrade the element compliance components using

$$D^{\eta} = 1 - \left[\frac{\sigma_{cr}}{E_{m}(\bar{\epsilon}_{f}^{\eta} - \bar{\epsilon}_{init}^{\eta})} \left(\frac{\bar{\epsilon}_{f}^{\eta}}{\bar{\epsilon}_{11}^{\eta}} - 1 \right) \right]$$
 (2)

where $\bar{\epsilon}_{\rm init}^{\eta}$ is the value of $\bar{\epsilon}_{11}^{\eta}$ when the initiation criterion ($\bar{\sigma}_{11}^{\eta} \geq \sigma_{\rm cr}$) is satisfied, $E_{\rm m}$ is the undamaged Young's modulus of the matrix. The damage parameter could take values between zero and one, where $D^{\eta}=0$ meant no damage had occurred. By contrast, a maximum damage level of one corresponded to a zero-stress state on the post-peak stress versus strain plot. Also, healing was inadmissible. Once the damage factor was computed, the relevant components of the compliance matrix were degraded [32, 34]. The progressive damage formulation was modeled in Abaqus/EXPLICIT solver with user-written subroutine VUMAT. The matrix strength $\sigma_{\rm cr}$ and a scaled-down fracture toughness $G_{\rm IC}$ corresponding to sub-micron length scale was prescribed to the material as listed in Table 1b.

A time-lapse of the virtual mechanical analysis for one 20 fiber composite microstructure ($v_f = 0.55$) is presented in Figure 3a, along with the stress versus strain plot. The stress versus strain plot manifested an initial linear elastic behavior up to point A followed by a significant pre-peak non-linearity (points A-D). The observed non-linear behavior was attributed to microcracking in the matrix material evident from the corresponding time-stamps on the contour plots. Following the peak (point D-E), the stresses in the microstructure progressively dropped until it had fully cracked (point E). The peak stress in the stress versus strain plot was regarded as the transverse composite strength σ_{22}^+ . The microstructure illustrated in Figure 3a registered a transverse strength $\sigma_{22}^+ = 21.1$ MPa. The contour plots of the maximum principal stresses, shown in Figure 3a, also highlight regions of high stress concentration. It is evident from the contour plots that stress localized in regions with dense fiber packing which then led to failure initiation and facilitated crack propagation. This phenomena was experimentally observed by Flores et al. [35] during transverse compression testing of composite micropillars. The final state at the end of the mechanical loading analysis of the five renditions of 20 fiber microstructure ($v_f = 0.55$) is presented in Figure 3b. Owing to the variations in the fiber packing. the crack propagated differently in each microstructure. Nevertheless, the crack consistently progressed through the densely packed regions of the microstructure, suggesting that fiber proximity and stress concentration significantly influence the transverse composite response [35]. Such sites are more susceptible to failure initiation which then facilitates crack growth in the microstructure. This knowledge was leveraged later in the study to correlate the transverse response of the composite microstructure to the geometrical arrangement of the fibers.

Composite microstructures of varying fiber volume fractions, illustrated in Figure 1, were analyzed as per the procedure described above. The results from the virtual mechanical tests are summarized in Figure 4 (black circles). The plot shows the predicted transverse composite strength as a function of the fiber volume fraction. Note that each circular data point on the plot is the average composite strength of five random microstructure renditions corresponding to a specific fiber volume fraction. For comparison purposes, the strength of the neat matrix that was obtained experimentally is also presented in Figure 4 (black diamond). It was evident that inclusion of fibers in the matrix caused the matrix to fail at a significantly lower strength of 23.6 ± 1.3 MPa instead of 64.1 MPa. As microstructures with denser fiber packing were analyzed, that is, as the fiber volume fraction increased from 0.24 to 0.6, the transverse strength of the analyzed microstructures further dropped from 23.6 ± 1.3 MPa to 20.6 ± 1.5 MPa. This drastic change in the transverse response can be associated with the increased fiber-to-fiber proximity with the fiber volume fraction. This close-fiber interaction, that results in stress concentration, and eventually affects the transverse strength of the composite, must be accounted for in the closed-form relation to accurately estimate the composite response. The subsequent sections leverage this knowledge to introduce and quantify a dimensionless stress concentration factor for developing the closed-form relation.

III. Closed-form Solution

The development of the proposed closed-form solution for transverse composite strength prediction will include the dependency on the elastic properties of the constituent phases, matrix strength, fiber volume fraction and the stress concentration in the microstructure,

$$\sigma_{22}^{+} = \sigma_{22}^{+} \left(E^{\text{m}}, E_{22}^{\text{f}}, \sigma_{\text{cr}}^{\text{m}}, \mathbf{SCF}_{22}^{+} \right)$$
 (3)

where, the transverse composite strength σ_{22}^+ was expressed as a function of the constituent fiber/matrix properties $E^{\rm m}$, $\sigma_{\rm cr}^{\rm m}$, $E_{22}^{\rm f}$; the fiber volume fraction $v_{\rm f}$; a stress concentration factor (SCF) for transverse loading SCF₂₂⁺ that accounted for the geometrical variations induced in the microstructure due to the inclusion of fibers. This SCF was expressed as a function of the shortest distance between a fiber pair δ , its orientation θ and the fiber volume fraction $v_{\rm f}$,

$$\mathbf{SCF}_{22}^{+} = \mathbf{SCF}_{\mathrm{I}}(\delta, \, \theta) \times \, \mathbf{SCF}_{\mathrm{II}}(\nu_{\mathrm{f}}) \tag{4}$$

Based on the findings of Huang et al. [10], Equation 3 was simplified to obtain an expression for transverse composite strength as,

$$\sigma_{22}^{+} = \frac{\sigma_{\text{cr}}^{\text{m}}}{\text{SCF}_{\text{I}} \times \text{SCF}_{\text{II}}}$$
 (5)

To determine the relevant expressions for the stress concentrations factors in Equation 5, a novel study was proposed, the details of which are described in the following sections.

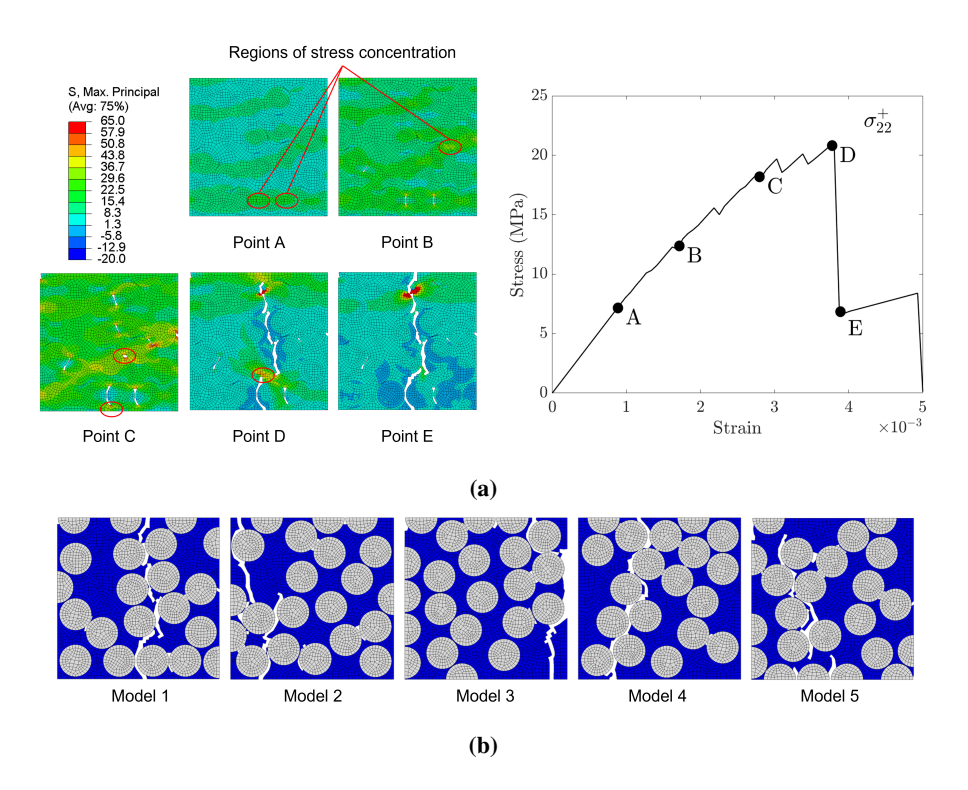


Fig. 3 (a) Time-lapse of the virtual test procedure and the corresponding stress σ vs. strain ϵ plot for a 20 fiber microstructure, (b) final state of all the realizations of the 20 fiber microstructure at the ned of the virtual mechanical loading analysis.

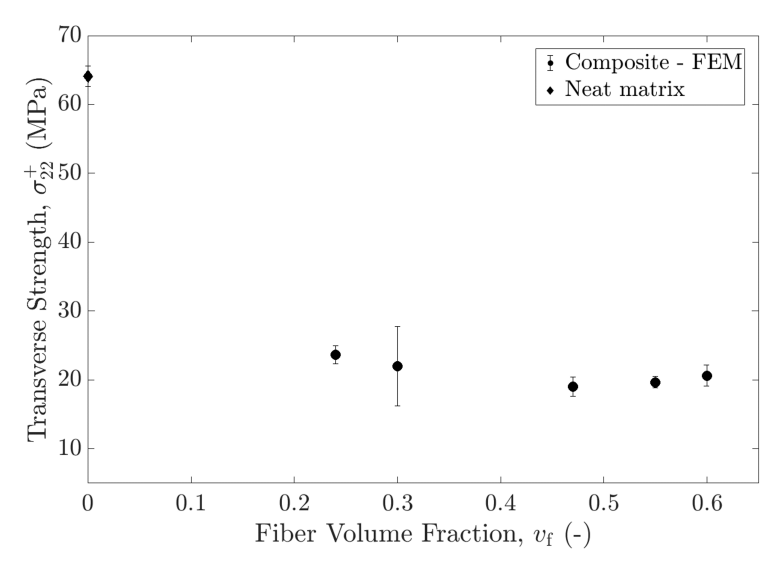


Fig. 4 Summary of the virtual mechanical analysis showing the transverse composite strength as a function of the fiber volume fraction.

A. Stress Concentration Factor

A stress concentration factor is defined as the ratio of the point-wise stresses in the proximity of a discontinuity within a continuum and the far-field/applied stress averaged over a boundary surface. In case of composite microstructures, a fiber inclusion within a matrix is a discontinuity which acts as a stress-riser. A simple linear-elastic analysis in FE yielded a SCF = 1.59 in a 1 fiber repeating unit cell (RUC) comprised of a glass fiber and epoxy matrix. The evaluation

of a global SCF in a multi-fiber microstructure becomes increasingly challenging since the stress field around a fiber is now non-uniform and is affected not only by the relative loading direction θ but also by the neighboring fibers within a certain proximity, δ . To determine the SCF in multi-fiber microstructures, a unique stress concentration analysis was proposed in this study.

First, the influence of introducing a neighboring fiber on the SCF was investigated with a 2 fiber model, the details of which are discussed in Section III.B. Following this, a correlation was established between the geometrical variations (δ and θ) in a multi-fiber microstructure and the SCF by virtue of the nearest neighbor statistical descriptor. This procedure is discussed in further detail in Section III.C.

B. Influence of fiber arrangement

The influence of introducing a second fiber on the SCF is investigated in the present section. Several 2 fiber models, with 14.1 μ m $\leq \delta \leq$ 20 μ m and 0° $\leq \theta \leq$ 90° (see Figure 5a), were generated in Abaqus. Assuming a linear elastic material definition, these models were subjected to transverse mechanical loads. The SCF in each case was then determined using the classic definition,

$$\mathbf{SCF}_{\mathrm{I}} = \frac{\sigma_{\mathrm{max}}}{\sigma_{\infty}} \tag{6}$$

where, σ_{max} is the maximum point stress, σ_{∞} is the the far-field/applied stress. The computed SCF_I for various combinations of δ and θ are shown in Figure 5a. For a constant value of $\delta = 14.1~\mu m$, highest stress concentration was observed when the fiber centers were oriented parallel to the loading direction ($\theta = 0^{\circ}$). The SCF_I rapidly decreased from 5.49 to 1.65 as θ increased to 60°. Beyond that, the SCF_I was unaffected by the orientation. By contrast, the SCF_I gradually reduced from 7.13 to 3.58 as the distance between the fibers δ increased from 14.1 μ m to 16 μ m while $\theta = 0^{\circ}$. The influence of relative fiber arrangement on the local stress concentration factor was clearly evident from Figure 5a. By analyzing an exhaustive combination of δ and θ , an interpolation function for SCF_I(δ , θ) was developed (see Figure 5b). This function was utilized in the subsequent section to determine the global SCF as a function of the geometrical variations (δ and θ) in the multi-fiber microstructures.

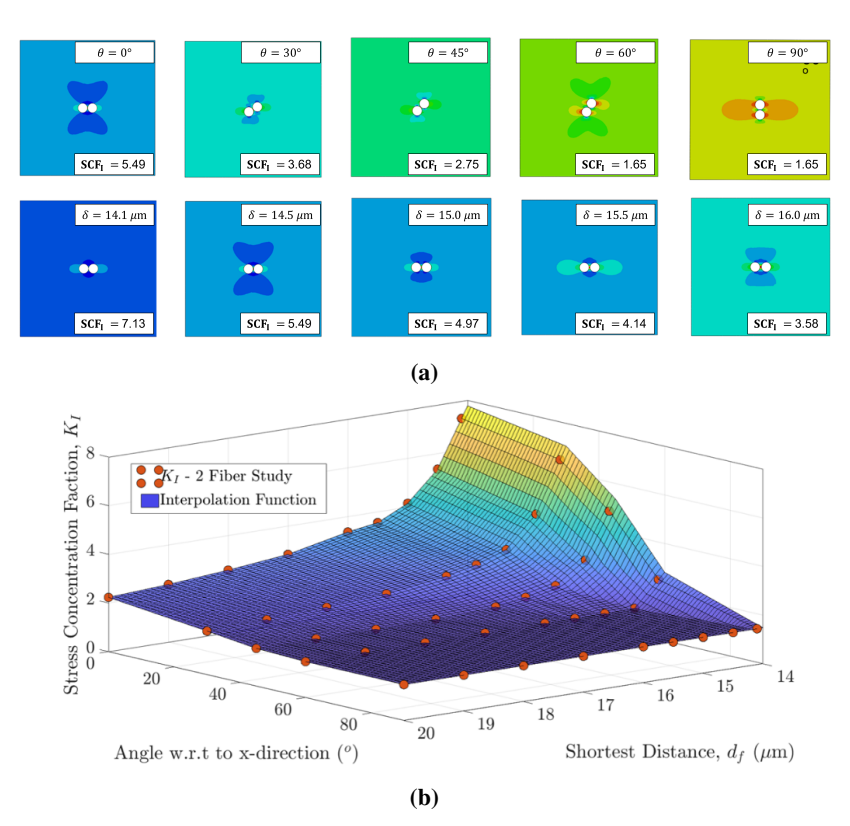


Fig. 5 (a) Variation in the fiber orientation θ (top row) and the distance between the fiber centers δ (bottom row) for the stress concentration study and (b) stress concentration factor SCF_I expressed as a function of δ and θ .

C. SCF in multi-fiber microstructures

To quantify the geometrical variations (δ and θ) in the multi-fiber microstructures analyzed in Section II and to establish a correlation with the global $\mathbf{SCF_I}$, the nearest neighbor statistical descriptor was utilized. For a given fiber center i in the microstructure, the algorithm identified its closest neighbor and measured the distance between the fiber centers δ^i along with the relative orientation θ^i with respect to the loading direction. This process was repeated for all the fiber centers in the microstructure. The mean shortest distance $\bar{\delta}$ and the corresponding mean orientation $\bar{\theta}$ was computed for each microstructure analyzed in Section II. Subsequently, the global $\mathbf{SCF_I}$ was computed with the help of the interpolation function $\mathbf{SCF_I}(\bar{\delta}, \bar{\theta})$. Figure 6 presents the global $\mathbf{SCF_I}$ as a function of the fiber volume fraction. Note that each data point on the plot is an average of five microstructure renditions with random fiber packing. The stress concentration factor increased with the fiber volume fraction. The observed trend was consistent with that exhibited by Figure 4, where the transverse strength dropped with an increase in the fiber volume fraction. Therefore, a correlation between the global $\mathbf{SCF_I}$ and the fiber volume fraction was established using a non-linear least-square regression fitting shown in Figure 6. This yielded a polynomial of second order

$$\mathbf{SCF}_{\mathbf{I}}(\delta, \theta) = \mathbf{SCF}_{\mathbf{I}}(v_{\mathbf{f}}) = 1 + av_{\mathbf{f}} + bv_{\mathbf{f}}^{2}$$
(7)

where, a = 2.422 and b = 1.091 are fitting parameters. Substituting $\sigma_{\rm cr}^{\rm m}$ from Table 1b, σ_{22}^{+} for each microstructure from Section II.B and Equation 7 into Equation 5, the expression for **SCF**_{II} was obtained as,

$$\mathbf{SCF}_{\mathrm{II}} = 1 + c\sqrt{v_{\mathrm{f}}} + dv_{\mathrm{f}} \tag{8}$$

where, c = 3.016 and d = -3.674 are fitting parameters. Equations 7 and 8 were substituted in Equation 5 to obtain the final closed-form solution for the transverse composite strength. The closed-form solution was able to accurately predict the transverse strength of the glass fiber/epoxy composite for a wide range of fiber volume fractions. It should be

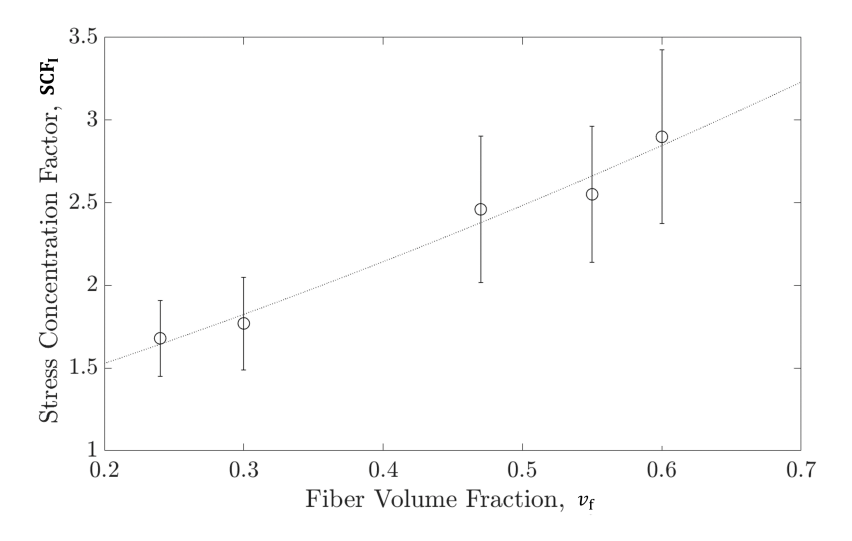


Fig. 6 Summary of the stress concentration analysis showing the global SCF_I as a function of the fiber volume fraction.

noted that Equations 5, 7 and 8 are material system specific and cannot be employed to predict the transverse composite response of a different constituent material system. This limitation is associated with the underlying assumption that the influence of the constituent fiber/matrix elastic properties on the SCF was implicitly accounted for in the data fitting process. The fitting parameters a - d would change if a different material system was analyzed. To determine these dependencies explicitly, and in the process, generalize the proposed closed-form model, several fiber/matrix combinations must be analyzed. This is being addressed in the ongoing work.

IV. Conclusions

This work provides a unique proof of concept to develop a closed-form solution for transverse composite strength prediction. A novel numerical approach was proposed in this study. Virtual mechanical tests were carried out on

composite microstructures with varying fiber volume fractions to predict their transverse strength. Stress concentration in composites due to fiber inclusion was explored and the global stress concentration factors in the analyzed microstructures were quantified using statistical descriptor. Finally, a material system specific closed-form solution was developed.

The proposed approach was based on certain fundamental assumptions that limited the prediction capabilities of the resulting closed-form solution. However, the proof of concept to develop a closed-form solution for transverse strength prediction is promising and needs further investigation. By analyzing several combinations of fiber/matrix systems, explicit dependencies can be established. The influence of constituent elastic properties on the SCF and the transverse composite response can be better understood and accounted for in the final expression. In the process, an improved and generalized closed-form solution can be developed. The presented methodology can be further expanded to incorporate the influence of manufacturing on the transverse composite response. This will be explored in a future study.

References

- [1] Galos, J., "Thin-ply composite laminates: a review," *Composite Structures*, Vol. 236, 2020, p. 111920. https://doi.org/10.1016/j.compstruct.2020.111920, URL https://www.sciencedirect.com/science/article/pii/S0263822319336943.
- [2] Liu, X., Furrer, D., Kosters, J., and Holmes, H., "Vision 2040: A Roadmap for Integrated, Multiscale Modeling and Simulation of Materials and Systems," Tech. rep., NASA, Mar. 2018. URL https://ntrs.nasa.gov/search.jsp?R=20180002010.
- [3] Huang, Z.-M., "On micromechanics approach to stiffness and strength of unidirectional composites.," *Journal of Reinforced Plastics and Composites*, 2018. https://doi.org/10.1177/0731684418811938, URL https://journals.sagepub.com/doi/10.1177/0731684418811938.
- [4] Huang, Z.-M., and Zhou, Y.-X., Strength of Fibrous Composites, Advanced Topics in Science and Technology in China, Springer-Verlag, Berlin Heidelberg, 2012. https://doi.org/10.1007/978-3-642-22958-9, URL https://www.springer.com/gp/book/9783642229572.
- [5] Reifsnider, K., Sendeckyj, G., Wang, S., Feng, W., Johnson, W., Stinchcomb, W., Pagano, N., Caruso, J., and Chamis, C., "Assessment of Simplified Composite Micromechanics Using Three-Dimensional Finite-Element Analysis," *Journal of Composites Technology and Research*, Vol. 8, No. 3, 1986, p. 77. https://doi.org/10.1520/CTR10326J, URL http://www.astm.org/doi/Link.cgi?CTR10326J.
- [6] Hashin, Z., "Analysis of Properties of Fiber Composites With Anisotropic Constituents," *Journal of Applied Mechanics*, Vol. 46, No. 3, 1979, pp. 543–550. https://doi.org/10.1115/1.3424603, URL https://asmedigitalcollection.asme.org/appliedmechanics/article/46/3/543/387554/Analysis-of-Properties-of-Fiber-Composites-With.
- [7] Mal, A. K., and Chatterjee, A. K., "The Elastic Moduli of a Fiber-Reinforced Composite," *Journal of Applied Mechanics*, Vol. 44, No. 1, 1977, pp. 61–67. https://doi.org/10.1115/1.3424015, URL https://asmedigitalcollection.asme.org/appliedmechanics/article/44/1/61/388822/The-Elastic-Moduli-of-a-Fiber-Reinforced-Composite.
- [8] Hashin, Z., and Rosen, B. W., "The Elastic Moduli of Fiber-Reinforced Materials," *Journal of Applied Mechanics*, Vol. 31, No. 2, 1964, pp. 223–232. https://doi.org/10.1115/1.3629590, URL https://asmedigitalcollection.asme.org/appliedmechanics/article/31/2/223/388899/The-Elastic-Moduli-of-Fiber-Reinforced-Materials.
- [9] Vignoli, L. L., Savi, M. A., Pacheco, P. M. C. L., and Kalamkarov, A. L., "Micromechanical analysis of transversal strength of composite laminae," *Composite Structures*, Vol. 250, 2020, p. 112546. https://doi.org/10.1016/j.compstruct.2020.112546, URL https://www.sciencedirect.com/science/article/pii/S0263822320310643.
- [10] Huang, Z.-M., and Xin, L.-M., "In situ strengths of matrix in a composite," *Acta Mechanica Sinica*, Vol. 33, No. 1, 2017, pp. 120–131. https://doi.org/10.1007/s10409-016-0611-1, URL https://doi.org/10.1007/s10409-016-0611-1.
- [11] Huang, Z.-M., and Liu, L., "Predicting strength of fibrous laminates under triaxial loads only upon independently measured constituent properties," *International Journal of Mechanical Sciences*, Vol. 79, 2014, pp. 105–129. https://doi.org/10.1016/j.ijmecsci.2013.08.010, URL http://www.sciencedirect.com/science/article/pii/S0020740313002221.
- [12] Lupăş, V., Țăranu, N., and Popoaei, S., "THEORETICAL STRENGTH PROPERTIES OF UNIDIRECTIONAL REINFORCED FIBER REINFORCED POLYMER COMPOSITES," 2013, p. 16.
- [13] Ghayoor, H., Hoa, S. V., and Marsden, C. C., "A micromechanical study of stress concentrations in composites," *Composites Part B: Engineering*, Vol. 132, 2018, pp. 115–124. https://doi.org/10.1016/j.compositesb.2017.09.009, URL https://www.sciencedirect.com/science/article/pii/S1359836816331146.

- [14] Liu, L., and Huang, Z.-M., "Stress concentration factor in matrix of a composite reinforced with transversely isotropic fibers," *Journal of Composite Materials*, Vol. 48, No. 1, 2014, pp. 81–98. https://doi.org/10.1177/0021998312469237, URL https://doi.org/10.1177/0021998312469237.
- [15] LLorca, J., González, C., Molina-Aldareguía, J. M., Segurado, J., Seltzer, R., Sket, F., Rodríguez, M., Sádaba, S., Muñoz, R., and Canal, L. P., "Multiscale Modeling of Composite Materials: a Roadmap Towards Virtual Testing," *Advanced Materials*, Vol. 23, No. 44, 2011, pp. 5130–5147. https://doi.org/10.1002/adma.201101683, URL https://onlinelibrary.wiley.com/doi/abs/10.1002/adma.201101683.
- [16] Hui, X., Xu, Y., Wang, J., and Zhang, W., "Microscale viscoplastic analysis of unidirectional CFRP composites under the influence of curing process," *Composite Structures*, Vol. 266, 2021, p. 113786. https://doi.org/10.1016/j.compstruct.2021.113786, URL https://www.sciencedirect.com/science/article/pii/S0263822321002476.
- [17] Huang, Z.-M., and Liu, L., "Assessment of composite failure and ultimate strength without experiment on composite," Acta Mechanica Sinica, Vol. 30, No. 4, 2014, pp. 569–588. https://doi.org/10.1007/s10409-014-0040-y, URL https://doi.org/10.1007/s10409-014-0040-y.
- [18] Maragoni, L., Carraro, P. A., and Quaresimin, M., "Development, validation and analysis of an efficient micro-scale representative volume element for unidirectional composites," *Composites Part A: Applied Science and Manufacturing*, Vol. 110, 2018, pp. 268–283. https://doi.org/10.1016/j.compositesa.2018.04.025, URL https://www.sciencedirect.com/science/article/pii/S1359835X18301647.
- [19] Sanei, S. H. R., Barsotti, E. J., Leonhardt, D., and Fertig, R. S., "Characterization, synthetic generation, and statistical equivalence of composite microstructures," *Journal of Composite Materials*, Vol. 51, No. 13, 2017, pp. 1817–1829. https://doi.org/10.1177/0021998316662133, URL https://doi.org/10.1177/0021998316662133.
- [20] Romanov, V., Lomov, S. V., Swolfs, Y., Orlova, S., Gorbatikh, L., and Verpoest, I., "Statistical analysis of real and simulated fibre arrangements in unidirectional composites," *Composites Science and Technology*, Vol. 87, 2013, pp. 126–134. https://doi.org/10.1016/j.compscitech.2013.07.030, URL http://www.sciencedirect.com/science/article/pii/S0266353813003047.
- [21] Wang, Z., Wang, X., Zhang, J., Liang, W., and Zhou, L., "Automatic generation of random distribution of fibers in long-fiber-reinforced composites and mesomechanical simulation," *Materials & Design*, Vol. 32, No. 2, 2011, pp. 885–891. https://doi.org/10.1016/j.matdes.2010.07.002, URL https://www.sciencedirect.com/science/article/pii/S026130691000436X.
- [22] Vaughan, T. J., and McCarthy, C. T., "A combined experimental-numerical approach for generating statistically equivalent fibre distributions for high strength laminated composite materials," *Composites Science and Technology*, Vol. 70, No. 2, 2010, pp. 291–297. https://doi.org/10.1016/j.compscitech.2009.10.020, URL https://www.sciencedirect.com/science/article/pii/ S0266353809003832.
- [23] Melro, A. R., Camanho, P. P., and Pinho, S. T., "Generation of random distribution of fibres in long-fibre reinforced composites," Composites Science and Technology, Vol. 68, No. 9, 2008, pp. 2092–2102. https://doi.org/10.1016/j.compscitech.2008.03.013, URL http://www.sciencedirect.com/science/article/pii/S0266353808001048.
- [24] Trias, D., Costa, J., Turon, A., and Hurtado, J. E., "Determination of the critical size of a statistical representative volume element (SRVE) for carbon reinforced polymers," *Acta Materialia*, Vol. 54, No. 13, 2006, pp. 3471–3484. https://doi.org/10.1016/j.actamat.2006.03.042, URL https://www.sciencedirect.com/science/article/pii/S1359645406002497.
- [25] Wongsto, A., and Li, S., "Micromechanical FE analysis of UD fibre-reinforced composites with fibres distributed at random over the transverse cross-section," Composites Part A: Applied Science and Manufacturing, Vol. 36, No. 9, 2005, pp. 1246–1266. https://doi.org/10.1016/j.compositesa.2005.01.010, URL https://www.sciencedirect.com/science/article/pii/S1359835X05000485.
- [26] Buryachenko, V. A., Pagano, N. J., Kim, R. Y., and Spowart, J. E., "Quantitative description and numerical simulation of random microstructures of composites and their effective elastic moduli," *International Journal of Solids and Structures*, Vol. 40, No. 1, 2003, pp. 47–72. https://doi.org/10.1016/S0020-7683(02)00462-6, URL https://www.sciencedirect.com/science/article/pii/S0020768302004626.
- [27] Byström, J., "Influence of the inclusions distribution on the effective properties of heterogeneous media," Composites Part B: Engineering, Vol. 34, No. 7, 2003, pp. 587–592. https://doi.org/10.1016/S1359-8368(03)00064-7, URL https://www.sciencedirect.com/science/article/pii/S1359836803000647.
- [28] Zeman, J., and Šejnoha, M., "Numerical evaluation of effective elastic properties of graphite fiber tow impregnated by polymer matrix," *Journal of the Mechanics and Physics of Solids*, Vol. 49, No. 1, 2001, pp. 69–90. https://doi.org/10.1016/S0022-5096(00)00027-2, URL https://www.sciencedirect.com/science/article/pii/S0022509600000272.

- [29] Gusev, A. A., Hine, P. J., and Ward, I. M., "Fiber packing and elastic properties of a transversely random unidirectional glass/epoxy composite," *Composites Science and Technology*, Vol. 60, No. 4, 2000, pp. 535–541. https://doi.org/10.1016/S0266-3538(99)00152-9, URL https://www.sciencedirect.com/science/article/pii/S0266353899001529.
- [30] Yang, S., Tewari, A., and Gokhale, A. M., "Modeling of Non-Uniform Spatial Arrangements of Fibers in a Ceramic Matrix Composite," Acta Materialia, Vol. 45, No. 7, 1997, pp. 3059–3069. https://doi.org/10.1016/S1359-6454(96)00394-1, URL https://www.sciencedirect.com/science/article/pii/S1359645496003941.
- [31] Carey, E., and Maiaru, M., "Randomization algorithm for the micromechanical modeling of fiber-reinforced Polymer Matrix Composites," *Proceedings of the American Society for Composites — Technical Conference*, Indiana, USA, 2017. https://doi.org/https://cdmhub.org/resources/1459.
- [32] Shah, S. P., and Maiarù, M., "Effect of Manufacturing on the Transverse Response of Polymer Matrix Composites," *Polymers*, Vol. 13, No. 15, 2021, p. 2491. https://doi.org/10.3390/polym13152491, URL https://www.mdpi.com/2073-4360/13/15/2491, number: 15 Publisher: Multidisciplinary Digital Publishing Institute.
- [33] Bažant, Z. P., and Oh, B. H., "Crack band theory for fracture of concrete," *Matériaux et Construction*, Vol. 16, No. 3, 1983, pp. 155–177. https://doi.org/10.1007/BF02486267, URL https://doi.org/10.1007/BF02486267.
- [34] Pineda, E. J., Bednarcyk, B. A., Waas, A. M., and Arnold, S. M., "Progressive failure of a unidirectional fiber-reinforced composite using the method of cells: Discretization objective computational results," *International Journal of Solids and Structures*, Vol. 50, No. 9, 2013, pp. 1203–1216. https://doi.org/10.1016/j.ijsolstr.2012.12.003, URL http://www.sciencedirect.com/science/article/pii/S0020768312005069.
- [35] Flores, M., Sesar, N., Wheeler, B., Sharits, A., and Mollenhauer, D., "Discrete Damage Modeling for a Transverse Compression Experiment of a Polymer Matrix Composite," *Proceedings of the American Society for Composites — Thirty-third Technical Conference*, Vol. 0, No. 0, 2018. https://doi.org/10.12783/asc33/26006, URL http://dpi-proceedings.com/index.php/asc33/article/view/26006, number: 0.